Amplified Protein Detection and Identification through DNA-Conjugated M13 Bacteriophage

Ju Hun Lee, Dylan W. Domaille, and Jennifer N. Cha*

Department of Nanoengineering and Materials Science and Engineering Program, University of California, San Diego, 9500 Gilman Drive M/C 0448, La Jolla, California 92093, United States

ABSTRACT

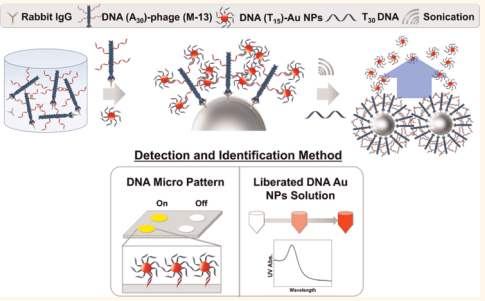

Sensitive protein detection and accurate identification continues to be in great demand for disease screening in clinical and laboratory settings. For these diagnostics to be of clinical value, it is necessary to develop sensors that have high sensitivity but favorable cost-to-benefit ratios. However, many of these sensing platforms are thermally unstable or require significant materials synthesis, engineering, or fabrication. Recently, we demonstrated that naturally occurring M13 bacteriophage can serve as biological scaffolds for engineering protein diagnostics. These viruses have five copies of the pIII protein, which can bind specifically to target antigens, and thousands of pVIII coat proteins, which can be genetically or chemically modified to react with signal-producing materials, such as plasmon-shifting gold nanoparticles (Au NPs). In this report, we show that DNA-conjugated M13 bacteriophage can act as inexpensive protein sensors that can rapidly induce a color change in the presence of a target protein yet also offer the ability to identify the detected antigen in a separate step. Many copies of a specific DNA oligonucleotide were appended to each virus to create phage-DNA conjugates that can hybridize with DNA-conjugated gold nanoparticles. In the case of a colorimetric positive result, the identity of the antigen can also be easily determined by using a DNA microarray. This saves precious resources by establishing a rapid, quantitative method to first screen for the presence of antigen followed by a highly specific typing assay if necessary.

KEYWORDS: M13 bacteriophage · protein · sensor · gold · nanoparticles · DNA · DNA micropattern

Many diseases, including prostate and breast cancer, continue to be a global public health problem.[1,2] To improve patient survival rates, advanced biomarker detection systems are necessary for early stage diagnosis, monitoring therapeutic response, and determining the efficacy of the treatment.[3−13] However, to obtain global applicability, these biomolecule detection systems must not only be sensitive but must also be easy to use, reliable, high-throughput, and inexpensive to manufacture. Within the biomedical community, chemically engineered viruses and virus-like particles (VLPs) have generated interest due to their potential for a variety of medical applications[14,15] including drug delivery,[16−18] serving as *in vitro* imaging scaffolds,[19−21] and platforms for biosensing.[22−25] One particular advantage for using viruses as scaffolds for imaging and detection is that they occur naturally and are readily produced by *E. coli*, which enables the generation of many virus copies without intensive fabrication. Furthermore, viruses are thermally and chemically robust,[17] and their coat protein composition can easily be modified synthetically or genetically, providing an inherent capacity for multivalent and orthogonal display.[21]

M13 bacteriophage is a particularly promising virus scaffold due to its well-established role in phage display technologies to identify particular peptide sequences that bind to specific targets.[26] M13 bacteriophage is a rodlike virus[27,28] in which the five minor capsid pIII proteins located at one end of the virus are involved in biological recognition, and the remaining major capsid pVIII proteins (~2700 copies per phage) are responsible only for the structural arrangement of bacteriophage.[29] Thus, the structure of the virus allows for the major capsid proteins to be chemically modified without disrupting its ability to bind a particular antigen. This approach was recently used to produce thiol-modified M13 bacteriophage that could cause Au nanoparticle aggregation, and the resulting plasmon resonance shifts acted as optical indicators of antigens in solution.[22] In addition to detecting a single type of antigen, multiplexed protein assays are also needed as they provide a means to identify and measure multiple biomarkers in solution and thereby

* Address correspondence to jencha@ucsd.edu.

Received for review April 9, 2012 and accepted May 15, 2012.

Published online May 15, 2012
10.1021/nn301565e

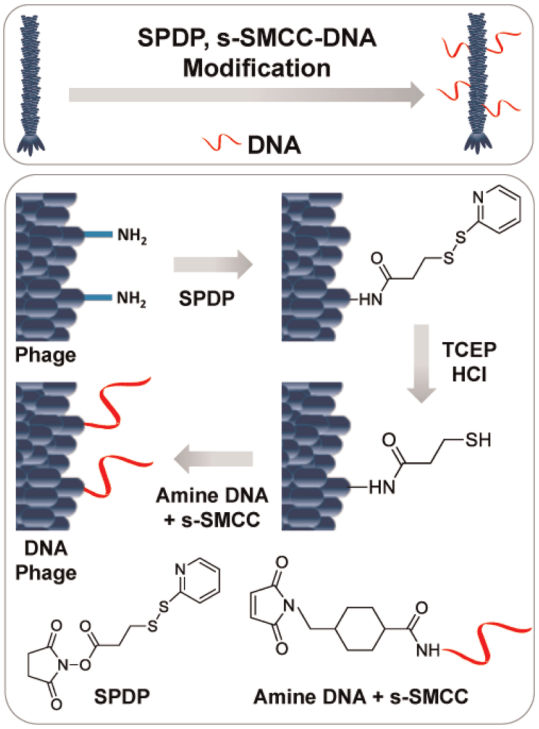

Scheme 1. Synthesis of DNA-modified M13 bacteriophage.

increase diagnostic accuracy.[2,30−32] In this report, we describe the synthesis of DNA-conjugated M13 bacteriophage and demonstrate its dual applicability for rapidly detecting and identifying antigens in solution with high sensitivity and accuracy.

RESULTS AND DISCUSSION

M13 bacteriophage that recognizes the model antigen antigoat rabbit immunoglobulin (IgG) was isolated through phage display.[22] Enzyme-linked immunosorbent assays (ELISAs) demonstrated that the viruses bound strongly and with high specificity to the target protein.[22] The phage did not bind to streptavidin or to surfaces conjugated with the incorrect antigen.[22] Next, the antigoat IgG binding phage was modified with multiple copies of A_{30} DNA. To install thiol nucleophiles on the phage coat, thiol groups were first incorporated onto the phage coat by reacting the phage with *N*-succinimidyl 3-[2-pyridyldithio]-propionate (SPDP) (Scheme 1) so that we could effectively conjugate the maleimide-derivatized DNA to the phage coat. The majority of the phage coat consists of 2700 copies of the same 50-amino acid peptide, which do not have any cysteine or disulfide bonds. While some disulfide bonds are buried in the minor capsid proteins of phage, the solvent-accessible SPDP groups are more accessible to tris(2-carboxyethyl)phosphine hydrochloride (TCEP-HCl). Upon reaction with TCEP, the pyridine 2-thione groups are removed to reveal free thiols on the phage. Finally, maleimide-bearing oligonucleotides (A_{30}), produced from amine-terminated A_{30} and sulfosuccinimidyl 4-[*N*-maleimidomethyl] cyclohexane-1-carboxylate (s-SMCC), were coupled with the thiol groups on the phage. While it is plausible that the amines on the phage could react with the maleimide-derivatized DNA, since the coupling was carried out at pH 7, the chemoselectivity was enhanced for the introduced thiol groups. In addition, the reaction rate of sulfhydryls with maleimides is 1000-fold faster than the reaction rate with amines;[33] thus, we could greatly favor the reaction of the thiols with the maleimide-DNA.

The resulting conjugate was characterized by matrix-assisted laser desportion ionization time-of-flight mass spectrometry (MALDI-TOF MS), UV−vis spectroscopy, and gel electrophoresis. The conversion ratio of SPDP-modified pVIII to total pVIII was quantitatively measured by MALDI-TOF MS. This synthetic approach led to the addition of approximately 1210 ± 85 SPDP groups per virus (Figure 1a). After Coomassie staining SDS PAGE gels, densitometric analysis was used to quantify the ratio of DNA-conjugated to unfunctionalized pVIII.[19,34] Using this approach, the phage-DNA conjugate prepared from 300 μM maleimide-modified DNA was determined to have 259 ± 19 DNAs per phage. (Figure 1b, Supporting Information, Table S1).

Next, to determine if chemical modification of the phage altered or inhibited its ability to bind its specific protein target, the DNA-conjugated phage was tested for binding to antigoat IgG through ELISA. As shown in Table 1, the DNA-conjugated phage showed similar binding affinities and specificities for antigoat IgG as compared to unmodified bacteriophage (Table 1). Although the relative ELISA signals from the DNA-conjugated phage were slightly lower than that from the native phage, which could be attributed to the DNA on the phage inhibiting anti-M13 antibody binding, the modification of the phage did not significantly alter the ELISA signals. Control assays showed that the DNA-conjugated phage bound neither the incorrect antigen biotinylated amylase nor the strepatvidin surfaces, indicating that DNA conjugation also did not affect the specificity of the phage.

To use the DNA-phage for both protein detection and identification, the A_{30}-DNA phage was incubated with varying concentrations of the model antigen, biotinylated antigoat rabbit IgG, and captured using streptavidin-coated magnetic beads. Unbound phage was removed by washing with PBST (PBS with 0.1% Tween) (Scheme 2). T_{15}-conjugated 10 nm Au nanoparticles (NPs) were then added to the magnetic bead pellets and vortexed to hybridize with the bound A_{30}-phage. After adding the DNA−Au NPs and removing the beads with a magnet, an immediate decrease in color was observed in the supernatant for samples containing antigen, indicating that some of the DNA-conjugated Au NPs had bound to the phage on the

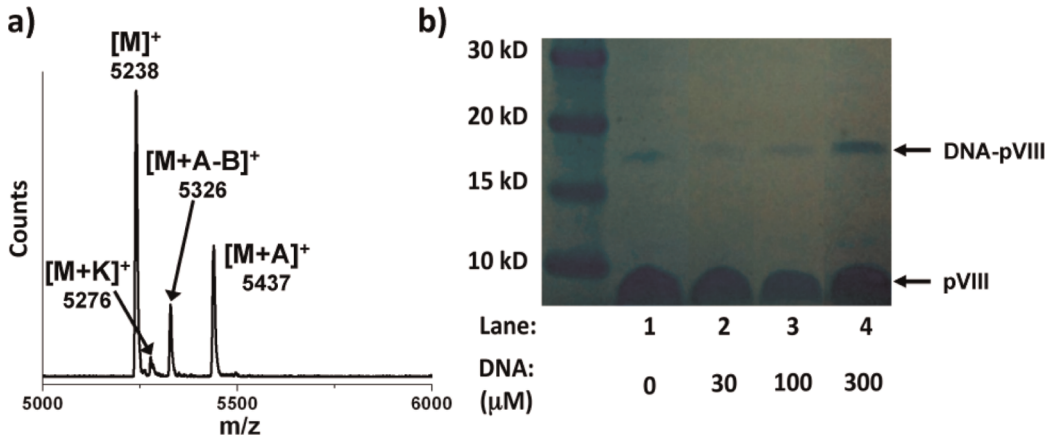

Figure 1. (a) MALDI-TOF MS of unmodified pVIII ($[M]^+$), pVIII + SPDP ($[M+A]^+$), and pVIII + SPDP−pyridine 2-thione ($[M+A-B]^+$). (b) Engineered DNA-M13 bacteriophage analyzed by SDS-PAGE. Lane 1 corresponds to native M13 bacteriophage. Lanes 2−4 correspond to phage reacted with different amounts of s-SMCC-derivatized DNA oligonucleotide (A_{30}).

TABLE 1. Comparison of Native and DNA-Phage Binding to Anti-goat IgG (model antigen) from Horse Radish Peroxidase-Conjugated Anti-M13 Antibodies, after Addition of ABTS[a]

	pure phage + antigen	pure phage + streptavidin	DNA phage + antigen	DNA phage + streptavidin
UV abs.	2.163	0.401	1.258	0.265

[a] The UV absorbance values at 410 nm. Antigoat IgG was used as model antigen.

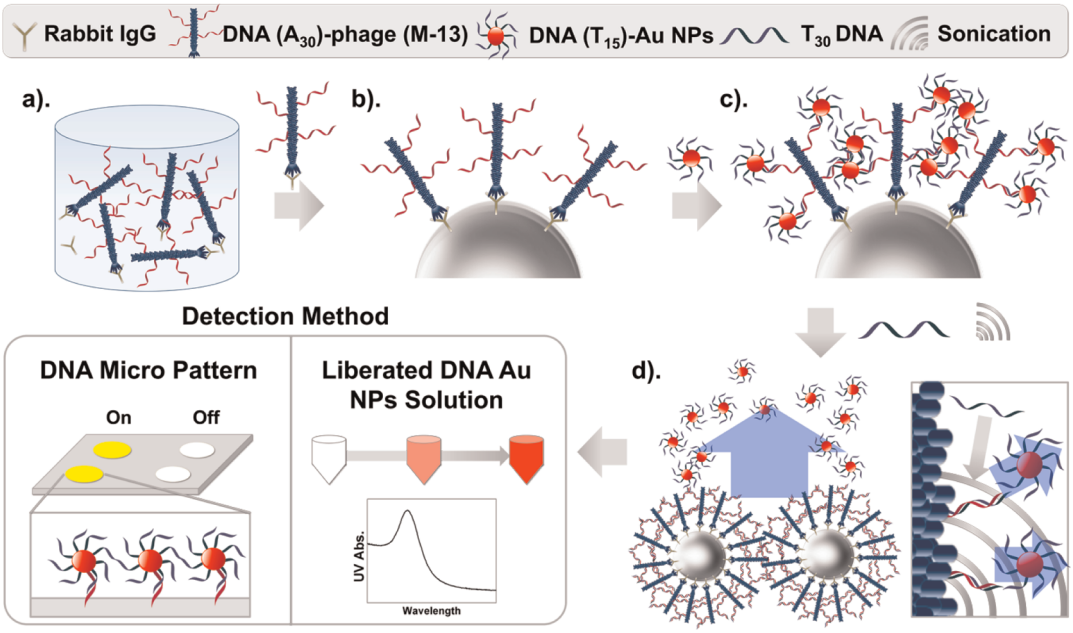

Scheme 2. Sensor Design with DNA-phage: (a) DNA-phage was reacted with the target antigen in the solution phase; (b) complexes of DNA (A_{30})-phage and antigen were captured with magnetic beads; (c) DNA (T_{15})−Au NPs were hybridized with captured DNA (A_{30})-phage; (d) DNA (T_{15})−Au NPs were competitively eluted with T_{30} DNA and sonication. Liberated DNA−Au NPs were analyzed by UV−vis spectroscopy values, and the sequence was identified with a DNA microarray.

beads (Supporting Information, Figure S1). With increasing amounts of antigen, more DNA−Au NPs bound to the magnetic beads, indicating that more phage bound to the beads at higher antigen amounts. Control assays using the incorrect antigen (biotinylated amylase and biotinylated bovine serum albumin (BSA)), the absence of antigen, or the absence of phage showed no color changes upon addition of Au NPs (Supporting Information, Figure S2).

To more precisely quantify the amount of antigen and to provide a method for identifying the specific antigen, the DNA−Au NPs were eluted back into solution, and the DNA sequences on the Au NPs were determined with DNA microarrays. To achieve this, the

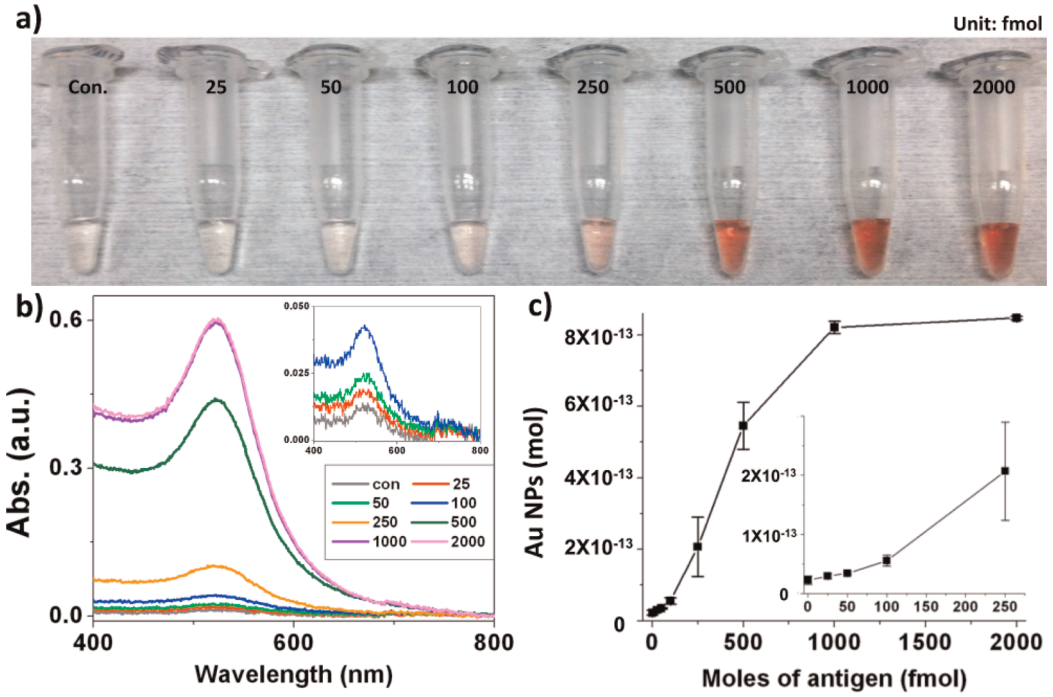

Figure 2. (a) After NP liberation, the supernatant showed an increase in color with an increase in antigen. (b) UV−vis spectra of liberated DNA−Au NPs. The inset shows UV−vis spectra of the lower antigen concentration regime. (c) Plot of total number of moles of liberated Au NPs *versus* antigen moles. Inset for lower amount of antigen. Error bars correspond to the standard deviation (n = 3).

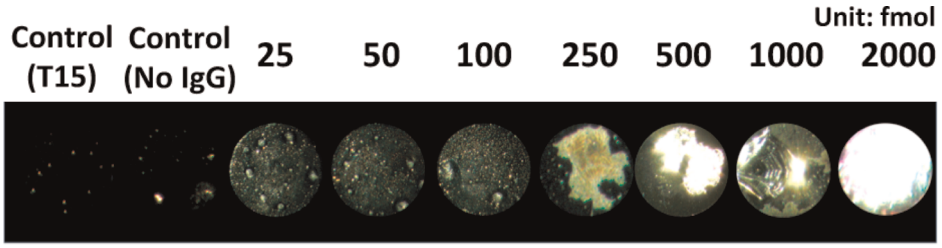

Figure 3. Dark field optical microscopy images of micropatterned DNA after hybridization with liberated DNA−Au NP.

T_{15}-DNA Au NPs bound to the A_{30}-phage were competitively eluted by adding excess T_{30} DNA, heating the solution, and allowing it to cool. Though this process released the bound DNA−Au NPs at lower concentrations of antigen (25−100 femtomoles), at higher antigen concentrations heating alone was found to be insufficient to dissociate any of the T_{15}-Au NPs. It is possible that at higher antigen concentrations, the higher DNA-phage loading on the magnetic beads led to more DNA−Au NP binding, which interfered with the diffusion of either the competitive T_{30} strand and/or the liberated DNA−Au NPs. To circumvent these problems, the samples were sonicated briefly to increase the rate and extent of nanoparticle dissociation. With even very brief heating and sonication, in the presence of T_{30}, the DNA−Au NPs were easily dissociated from the phage at all antigen concentrations studied (Supporting Information, Figure S3). UV−vis measurements of the supernatants showed that increasing amounts of T_{15}-Au NPs were eluted with increasing amounts of antigen, with a detection limit of 25 fmole antigen (Figure 2). Control assays using the incorrect antigen (biotinylated amylase and biotinylated bovine serum albumin (BSA)), the absence of antigen, or the absence of phage showed almost no color of Au NPs as well as relatively weak or negligible UV−vis signal in the liberated solutions (Supporting Information, Figure S4). Alternatively, the UV−vis absorption values were converted to moles of NPs, and this was used as a method to quantify the moles of antigen in solution (Figure 2c). The error bars in Figure 2c corresponded to the standard deviation of the assay from three independent preparations of the conjugate; thus, the variability inherent in the preparation of each batch is included in the uncertainty of each value.

To identify the DNA sequence on the Au NPs and therefore the antigen, after competitive elution, excess T_{30} DNA was removed by microcentrifuge filtration. The filtered and concentrated DNA−Au NPs were then adsorbed to printed DNA microarrays, and after

washing away excess nanoparticles with saline sodium citrate (SSC) buffer, the T_{15} -Au NPs were easily detected on printed arrays of A_{15} (Figure 3). Printed control arrays of T_{15} (Figure 3, Control 1) showed no binding of the T_{15}-Au NPs, demonstrating the high binding specificity and validating the use of DNA microarrays to identify the DNA sequence and, therefore, the antigen in solution.

CONCLUSION

We have demonstrated that M13 bacteriophage can be modified with multiple DNA oligonucleotides to generate a single bioanalytical platform that not only enables the facile and rapid detection of antigens in solution but also provides a system for protein identification. Because every virus is composed of thousands of the coat pVIII protein, none of which is responsible for binding the antigen, it is possible to chemically conjugate distinct moieties onto a single virus scaffold that play dual roles in protein sensing and identification. Interactions between the DNA-phage and DNA–Au NPs led to observation of immediate color changes, which can first be used optically or spectroscopically to detect the presence of an antigen in solution. In addition, the same DNA-phage platform can be used to identify the types of antigens in solution by competitively eluting the DNA–Au NPs from the phage and adsorbing the particles to printed DNA microarrays. Because each phage recognizes 1–2 antigens yet can bind to hundreds of DNA–Au NPs through the pendant DNA chains on the virus' pVIII proteins, these sensors are extremely sensitive, easy to use, can provide both protein detection and identification in an extremely high throughput manner, and are ultimately inexpensive to manufacture. Future work will involve studying the use of DNA-phage for multiplexing with clinically relevant biomarkers.

MATERIALS AND METHODS

Phage Display. Commercial M13 bacteriophage libraries (New England Biolabs) were used for phage display screening. Phage libraries were reacted in solution with 10 pmol of the model antigen, biotinylated rabbit IgG (Sigma Aldrich), captured using streptavidin-coated magnetic Dynabeads, and washed with TBS and Tween-20 (TBST). Bound phage was eluted with 0.2 M glycine–HCl buffer (pH 2.2) with BSA and neutralized with 1 M Tris buffer (pH 9.1). Three rounds of screening were run, at which point individual phage plaques were subjected to DNA sequencing. After three rounds of screening, the consensus peptide sequence DHVRSSSISSLT was obtained.

DNA Conjugation of Phage. Amine-terminated oligonucleotides (A_{30}) were attached to the phage by first reacting the pVIII protein amine groups with *N*-succinimidyl 3-(2-pyridyldithio) propionate (SPDP, Thermo scientific). SPDP (200 μM) was reacted with 1.5 mg/mL phage in pH 7.4 PBS at room temperature (RT) for 1 h. Excess SPDP was removed by precipitating the phage with PEG/NaCl solution (20% w/v PEG/2.5 M NaCl). The SPDP-modified phage was next reacted with excess tri(2-carboxyethyl)phosphine hydrochloride (TCEP-HCl, Thermo scientific) for 30 min to reduce the disulfide bridge. The reaction mixture was desalted twice. Concurrently and in separate vials, amine-terminated oligonucleotides in PBS (pH 7) were reacted with a 10-fold molar excess of sulfo-succinimidyl 4-[*N*-maleimidomethyl]cyclohexane-1-carboxylate (s-SMCC) at RT for 40 min, and the resulting maleimide-modified DNA was precipitated in ethanol and centrifuged to remove excess s-SMCC. Deprotected thiol-modified phage and maleimide-modified DNA were then reacted at RT in 1× PBS overnight. The DNA-modified phage was purified by centrifuge filtration.

MALDI-TOF for Characterization of DNA Modified Phage. For characterization of SPDP modified phage, 2 μL of the SPDP phage solution (2 mg/mL) was denatured with 3 M guanidine chloride for 5 min at RT, purified with a Millipore C18-ZipTip, and characterized with a Bruker MALDI mass spectrometer. 2,4,6-Trihydroxyacetophenone monohydrate/ammonium citrate solution (50 mg/mL:12.5 mg/mL in MeOH) was used as the matrix.

DNA Microarrays. Epoxy-coated glass substrates (Arrayit) were used to generate the DNA micropatterns. Amine-terminated DNA (75 μM of oligonucleotides with 25 v/v % Spotting Solution Plus) was printed on the epoxy glass substrate, immobilized for 1–2 h in a humidified chamber, and baked at 60 °C for 30 min. The patterned glass substrates were used immediately or stored under dry and dark conditions at room temperature. The printed micro-A_{15}-patterned glass was successively washed with 0.1% Triton X-100 for 5 min and DI water for 1 min and blocked (12.5 mM ethanolamine, 0.025% SDS in 25 mM Tris, pH 9.0) at 50 °C for 15 min.

DNA-Phage-Based Protein Detection and Identification Assay. A 600 fmol portion of DNA-phage was reacted with varying amounts of biotinylated antigoat IgG. The DNA-phage-antibody complexes were captured with streptavidin-coated magnetic beads (Dynabeads) and washed with 1× PBS containing Tween-20 (0.1%). DNA-conjugated (T_{15}) 10 nm Au NPs were reacted with the A_{30} DNA-phage on magnetic beads in 1× PBS. The supernatants were collected, and the absorption at 520 nm was monitored to determine how many DNA–Au NPs were bound. The bound 10 nm DNA–Au NPs were eluted by competitive elution with DNA (T_{30}) at 95 °C for 10 min. After heating and cooling, the samples were briefly sonicated. Liberated 10 nm DNA Au NPs were purified with a 100 K MWCO filter to remove remaining T_{30} and to concentrate the solutions. The 10 nm DNA Au NPs were adsorbed to DNA microarrays in 50 mM $MgCl_2$ for 1 h in a humidified chamber. After hybridization, the substrate was washed sequentially with 2× SSC with 0.1% SDS, 2× SSC, and 1× SSC.

Conflict of Interest: The authors declare no competing financial interest.

Acknowledgment. We acknowledge support from the NSF CAREER (DMR-1056808) and the Office of Naval Research (Award No. N00014-09-01-0250). We thank A. Goodwin and M. Brasino for valuable discussions.

Supporting Information Available: Additional figures as described in the text. This material is available free of charge *via* the Internet at http://pubs.acs.org.

REFERENCES AND NOTES

1. Siegel, R.; Ward, E.; Brawley, O.; Jemal, A. Cancer Statistics, 2011, The Impact of Eliminating Socioeconomic and Racial Disparities on Premature Cancer Deaths. *CA- Cancer J. Clin.* **2011**, *61*, 212–236.
2. Torthill, I. E. Biosensors for Cancer Markers Diagnosis. *Semin. Cell Dev. Biol.* **2009**, *20*, 55–62.
3. Peeling, R. W; Holmes, K. K.; Mabey, D; Ronald, A. Rapid Tests for Sexually Transmitted Infections (STIs): The Way Forward. *Sex. Transm. Infect.* **2006**, *82*, v1–v6.

4. Xia, F.; Zuo, X.; Yang, R.; Xiao, Y.; Kang, D.; Vallée-Bélisleb, A.; Gong, X.; Yuen, J. D.; Hsu, B. B. Y.; Heeger, A. J.; *et al*. Colorimetric Detection of DNA, Small Molecules, Proteins, and Ions Using Unmodified Gold Nanoparticles and Conjugated Polyelectrolytes. *Proc. Natl. Acad. Sci.* **2010**, *107*, 10837–10841.
5. Martinez, A. W.; Phillips, S. T.; Butte, M. J.; Whitesides, G. M. Patterned Paper as a Platform for Inexpensive, Low-Volume, Portable Bioassays. *Angew. Chem., Int. Ed.* **2007**, *46*, 1318–1320.
6. Martinez, A. W.; Phillips, S. T.; Whitesides, G. M.; Carrilho, E. Diagnostics for The Developing World: Microfluidic Paper-Based Analytical Devices. *Anal. Chem.* **2010**, *82*, 3–10.
7. Rosi, N. L.; Mirkin, C. A. Nanostructures in Biodiagnostics. *Chem. Rev.* **2005**, *105*, 1547–1562.
8. Hahm, J.; Lieber, C. M. Direct Ultrasensitive Electrical Detection of DNA and DNA Sequence Variations Using Nanowire Nanosensors. *Nano Lett.* **2004**, *4*, 51–54.
9. Kim, D.; Daniel, W. L.; Mirkin, C. A. Microarray-Based Multiplexed Scanometric Immunoassay for Protein Cancer Markers Using Gold Nanoparticle Probes. *Anal. Chem.* **2009**, *81*, 9183–9187.
10. Xiang, Y.; Xie, M.; Bash, R.; Chen, J. J. L.; Wang, J. Ultrasensitive Label-Free Aptamer-Based Electronic Detection. *Angew. Chem., Int. Ed.* **2007**, *119*, 9212–9214.
11. Borisov, S. M.; Wolfbeis, O. S. Optical Biosensors. *Chem. Rev.* **2008**, *108*, 423–461.
12. Medintz, I. L; Clapp, A. R.; Mattoussi, H.; Goldman, E. R.; Fisher, B.; Mauro, J. M. Self-Assembled Nanoscale Biosensors Based on Quantum Dot FRET Donors. *Nat. Mater.* **2003**, *2*, 630–638.
13. Cui, Y.; Wei, Q.; Park, H.; Lieber, C. M. Nanowire Nanosensors for Highly Sensitive and Selective Detection of Biological and Chemical Species. *Science* **2001**, *293*, 1289–1292.
14. Mateu, M. G. Virus Engineering: Functionalization and Stabilization. *Protein Eng., Des. Sel.* **2011**, *24*, 53–63.
15. Yildiz, I.; Shukla, S.; Steinmetz, N. F. Applications of Viral Nanoparticles in Medicine. *Curr. Opin. Biotechnol.* **2011**, *22*, 901–908.
16. Ngweniform, P.; Abbineni, G.; Cao, B.; Mao, C. Self-Assembly of Drug-Loaded Liposomes on Genetically Engineered Target-Recognizing M13 Phage: A Novel Nanocarrier for Targeted Drug Delivery. *Small* **2009**, *5*, 1963–1969.
17. Mao, C.; Liu, A.; Cao, B. Virus-Based Chemical and Biological Sensing. *Angew. Chem., Int. Ed.* **2009**, *48*, 6790–6810.
18. Yacoby, I.; Bar, H.; Benhar, I. Targeted Drug-Carrying Bacteriophages as Antibacterial Nanomedicines. *Antimicrob. Agents Chemother.* **2007**, *51*, 2156–2163.
19. Tong, G. J.; Hsiao, S. C.; Carrico, Z. M.; Francis, M. B. Viral Capsid DNA Aptamer Conjugates as Multivalent Cell-Targeting Vehicles. *J. Am. Chem. Soc.* **2009**, *131*, 11174–11178.
20. Robertson, K. L.; Soto, C. M.; Archer, M. J.; Odoemene, O.; Liu, J. L. Engineered T4 Viral Nanoparticles for Cellular Imaging and Flow Cytometry. *Bioconjugate Chem.* **2011**, *22*, 595–604.
21. Li, K; Chen, Y.; Li, S.; Nguyen, H. G.; Niu, Z.; You, S.; Mello, C. M.; Lu, X.; Wang, Q. Chemical Modification of M13 Bacteriophage and Its Application in Cancer Cell Imaging. *Bioconjugate Chem.* **2010**, *21*, 1369–1377.
22. Lee, J. H.; Cha, J. N. Amplified Protein Detection through Visible Plasmon Shifts in Gold Nanocrystal Solutions from Bacteriophage Platforms. *Anal. Chem.* **2011**, *83*, 3516–3519.
23. Goldman, E. R.; Pazirandeh, M. P.; Mauro, J. M.; King, K. D.; Frey, J. C.; Anderson, G. P. Phage-Displayed Peptides as Biosensor Reagents. *J. Mol. Recognit.* **2000**, *13*, 382–387.
24. Petrenko, V. A.; Vodyanoy, V. J. Phage Display for Detection of Biological Threat Agents. *J. Microbiol. Methods* **2003**, *53*, 253–262.
25. Arter, J. A.; Taggart, D. K.; Mcintire, T. M.; Penner, R. M.; Weiss, G. A. Virus-PEDOT Nanowires for Biosensing. *Nano Lett.* **2010**, *10*, 4858–4862.
26. Smith, G. P.; Petrenko, V. A. Phage Display. *Chem. Rev.* **1997**, *97*, 391–410.
27. Barbas III, C. F.; Burton, D. R.; Scott, J. K.; Silverman, G. J. *In Phage Display. A Laboratory Manual*; Cold Spring Harbor Laboratory Press: New York, 2001; pp 1.1−16.
28. Kehoe, J. W.; Kay, B. K. Filamentous Phage Display in the New Millennium. *Chem. Rev.* **2005**, *105*, 4056–4072.
29. Hemminga, M. A.; Vos, W. L.; Nazarov, P. V.; Koehorst, R. B. M.; Wolfs, C. J. A. M.; Spruijt, R. B.; Stopar, D. Viruses: Incredible Nanomachines. New Advances with Filamentous Phages. *Eur. Biophys. J.* **2010**, *39*, 541–550.
30. Stoeva, S. I.; Lee, J.; Smith, J. E.; Rosen, S. T.; Mirkin, C. A. Multiplexed Detection of Protein Cancer Markers with Biobarcoded Nanoparticle Probes. *J. Am. Chem. Soc.* **2006**, *128*, 8378–8379.
31. Geißler, D.; Charbonniere, L. J.; Ziessel, R. F.; Butlin, N. G.; Löhmannsröben, H.; Hildebrandt, N. Quantum Dot Biosensors for Ultrasensitive Multiplexed Diagnostics. *Angew. Chem., Int. Ed.* **2010**, *49*, 1396–1401.
32. Bailey, R. C.; Kwong, G. A.; Radu, C. G.; Witte, O. N.; Heath, J. R. DNA-Encoded Antibody Libraries: A Unified Platform for Multiplexed Cell Sorting and Detection of Genes and Proteins. *J. Am. Chem. Soc.* **2007**, *129*, 1959–1967.
33. Hermanson, G. T. *Bioconjugate Techniques*, 2nd ed.; Academic Press: San Diego, CA, 2008; pp 183−184.
34. Stephanopolous, N.; Tong, G. J.; Hsiao, S. C.; Francis, M. B. Dual-Surface Modified Capsids for Targeted Delivery of Photodynamic Agents to Cancer Cells. *ACS Nano* **2010**, *4*, 6014–6020.